minerals

MDPI

Article

Effect of Ferric Ions on Sulfidization Flotation of Oxidize Digenite Fine Particles and Their Significance

Jiwei Xue [1,2], Dawei Ren [1], Sen Wang [1], Xianzhong Bu [1,*], Zhenguo Song [2], Chen Zhao [2] and Tong Chen [1]

[1] School of Resources Engineering, Xi'an University of Architecture and Technology, Xi'an 710055, China; xjw635171816@xauat.edu.cn (J.X.); rdw0011@163.com (D.R.); wangsne@163.com (S.W.); chentong@xauat.edu.cn (T.C.)

[2] State Key Laboratory of Mineral Processing, Beijing 100260, China; Songzhenguo@bgrimm.com (Z.S.); zhaochen@bgrimm.com (C.Z.)

* Correspondence: buxianzhong@xauat.edu.cn; Tel.: +86-181-9283-3797

Abstract: Digenite fine particles are easily oxidized and ferric ions (Fe^{3+}) commonly exist in the flotation pulp of digenite. This study investigated the effect of Fe^{3+} on the sulfidization flotation of oxidized digenite fine particles using sodium butyl xanthate (SBX) as a collector. The results of microflotation experiments show that the flotation rate and recovery of oxidized digenite fine particles can be improved by adding Na_2S and SBX, whereas the existence of large amounts of Fe^{3+} is not beneficial for the sulfidization flotation of digenite. The results of Fe^{3+} adsorption, zeta potential, and contact angle measurements indicate that Fe^{3+} can be adsorbed on the digenite surface mainly in the form of $Fe(OH)_3$, which hinders the adsorption of SBX and significantly reduces the surface hydrophobicity of digenite. X-ray photoelectron spectroscopy analysis further suggests that the poor surface hydrophobicity of digenite in the presence of Fe^{3+} is due to the production of large amounts of hydrophilic iron and copper oxides/hydroxides on the surface. Furthermore, optical microscopy analysis shows that these hydrophilic species effectively disperse digenite fine particles in the pulp, which eventually leads to the poor floatability of digenite. Therefore, it is necessary to reduce the amount of Fe^{3+} present in the pulp and adsorbed on digenite surface before sulfidization to realize effective separation of oxidized digenite fine particles and iron sulfide minerals.

Keywords: oxidized digenite fine particles; ferric ions; sulfidization flotation; adsorption; surface hydrophobicity

Citation: Xue, J.; Ren, D.; Wang, S.; Bu, X.; Song, Z.; Zhao, C.; Chen, T. Effect of Ferric Ions on Sulfidization Flotation of Oxidize Digenite Fine Particles and Their Significance. *Minerals* **2021**, *11*, 305. https://doi.org/10.3390/min11030305

Academic Editor: Kirsten Claire Corin

Received: 4 March 2021
Accepted: 15 March 2021
Published: 16 March 2021

1. Introduction

Copper is an important nonferrous metal and has extensive applications in the fields of medicine, machine manufacturing, and electrical and national defense industries [1,2]. Copper sulfide minerals are the main source of copper, and they are usually recovered by flotation methods. For coarse particles, copper sulfide minerals are easily floated by the addition of sulfhydryl collectors. However, once the particles become fine, it is extremely challenging to effectively recover the minerals by flotation. This is because the fine particles have the characteristics of low collision probability with the bubble, high surface energy, and large specific surface, which require a high consumption of collectors [3–6]. In addition, the fine particles are more easily oxidized when exposed to oxygen and water during mineral processing. After heavy oxidation, large amounts of hydrophilic copper oxides/hydroxides cover the surface and prevent the effective recovery of minerals. Therefore, some valuable fine particles are usually discarded in the tailings, which leads to a loss of copper.

In flotation practice, various metal ions, known as unavoidable ions, always exist in the pulp. These metal ions can enhance or inhibit the adsorption of collectors on mineral surfaces, thus influencing the flotation of the target minerals. In the flotation of base metal sulfide minerals, ferric ions (Fe^{3+}) are common unavoidable ions, mainly originating from the surface oxidation and dissolution of iron sulfide minerals, electrochemical corrosion of

the grinding media, and release of fluid inclusions [7–9]. Previous studies have demonstrated that Fe^{3+} species can be adsorbed onto the surface of unoxidized copper sulfide minerals, thus preventing the flotation of minerals. Peng et al. [10] suggested that iron oxidation species from a mild steel grinding medium could result in the low flotation recovery of chalcopyrite. Ma et al. [11] showed that Fe^{3+} can significantly suppress the flotation of digenite at pH 3–11 when ammonium dibutyl dithiophosphate is used as the collector; this can be attributed to the adsorption of $Fe(OH)_3$ precipitate on the surface. However, when copper sulfide minerals are heavily oxidized, the adsorption of Fe^{3+} and its effect on the following flotation of minerals is still indefinite.

It is well known that presulfidization before the addition of sulfhydryl collectors is necessary for the effective recovery of base metal oxide minerals, such as malachite [12,13], azurite [14], and cerussite [15]. During sulfidization, HS^- reacts with the base metal ions on or dissolved from the surface to produce the base metal copper sulfide-like minerals, thus increasing the effectiveness of the collectors and the floatability of the base metal oxide minerals. Based on this principle, sulfidization has also been widely used to treat oxidized sulfide minerals, such as digenite, chalcopyrite, and pyrite [16–19]. Therefore, in this study, the sulfidization technology was applied to try to restore the floatability of oxidized digenite fine particles, and then the effect of Fe^{3+} on its sulfidization flotation was investigated. Flotation was performed in batch flotation tests to determine the effect of Fe^{3+} on the flotation rate and recovery of minerals. The underlying mechanism was studied in detail through Fe^{3+} adsorption experiments, zeta potential measurements, contact angle measurements, X-ray photoelectron spectroscopy (XPS), and optical microscopy analysis. This study is expected to provide further clarification regarding the effective sulfidization flotation of fine particles of oxidized copper sulfide mineral.

2. Materials and Methods

2.1. Mineral Samples and Reagents

Digenite samples are from Fujian Province in China. Lump samples were crushed, hand-selected, dry ground in a porcelain ball mill, and then screened to obtain fine particles (−20 μm) for oxidation and microflotation experiments. The samples were oxidized by the natural oxidation method, in which the samples were kept flat on glass dishes and exposed to air for 120 days at a temperature of approximately 25 °C and relative humidity of 60%.

Sodium normal butyl xanthate (SBX) with a purity of 95% was used as the collector of digenite. Ferric chloride hexahydrate ($FeCl_3 \cdot 6H_2O$) and sodium sulfide nonahydrate ($Na_2S \cdot 9H_2O$) were used as sources of Fe^{3+} and S^{2-}, respectively. Hydrochloric acid (HCl) and sodium hydroxide (NaOH) were used as pH regulators. Terpenic oil was used as the frother. $FeCl_3 \cdot 6H_2O$, $Na_2S \cdot 9H_2O$, HCl, and NaOH were all of analytical grade. SBX and terpenic oil were of industrial grade. Deionized (DI) water with a resistivity of 18.3 MΩ·cm was used in all the experiments.

2.2. Microflotation Experiments

The microflotation experiments were conducted using an XFD laboratory flotation machine with an impeller speed of 1752 r/min. During flotation, digenite (5.0 g) was placed in the flotation cell, and then 50 mL of DI water was added to the flotation cell for 3 min. Then, HCl or NaOH was added to regulate the pulp pH to the required value. Subsequently, $FeCl_3$ (if needed), Na_2S, SBX, and terpenic oil were sequentially added to the pulp and conditioned for 3 min each, except terpenic oil, which was conditioned for 1 min. The dosage of terpenic oil was fixed at 40 mg/L throughout the experiments. Finally, the froth products were collected at 0.2, 0.4, 0.6, 0.8, 1.0, 1.5, 2.0, and 3.0 min. After flotation, the froth products and tailings were filtered, dried, weighed, and analyzed. The obtained data were fitted using the classical first-order flotation kinetic model and expressed as follows:

$$R(t) = R_\infty \times [1 - \exp(-k \times t)] \quad (1)$$

where $R(t)$ represents the floatability at a certain flotation time t (min), R_∞ represents the infinite recovery, and k represents the flotation rate constant (min^{-1}).

In many cases, the adjusted flotation rate constant (K) considering both the parameters of R_∞ and k is more suitable for comparison with the flotation rate under different conditions [20–22]. In this study, the flotation rate was evaluated using the K value, and the formula is expressed as follows:

$$K = k \times R_\infty / 100 \quad (2)$$

2.3. Adsorption Experiments

The amount of Fe^{3+} adsorbed on the surface of digenite was measured using inductively coupled plasma-optical emission spectroscopy (Agilent 5110, Agilent Technologies Co., Ltd., Santa Clara, CA, USA). During sample preparation, 5 g of digenite samples was mixed with 50 mL of DI water and magnetically stirred in a beaker for 3 min. Then, the desired pH regulator and $FeCl_3$ were added to the solution and stirred for 10 min. The samples and solutions were separated via centrifugation. The residual Fe concentration in the solutions was determined by referring to a standard curve for absorbance as a function of the Fe concentration. The amount of Fe^{3+} adsorbed was calculated by the difference from the initial concentration [23].

2.4. Zeta Potential Measurements

The zeta potential values of digenite under different conditions were obtained using a Malvern Instruments Nano-ZS90 (Malvern Instruments, Malvern, UK) zeta potential analyzer at approximately 25 °C. Potassium nitrate was used to maintain the ionic strength at 1×10^{-3} mol/L [24]. During the measurements, 20 mg of digenite samples was mixed with 50 mL of DI water with and without the addition of $FeCl_3$, Na_2S, and SBX, the solutions of which were magnetically stirred for 5 min. Subsequently, the pH was adjusted using 0.1 mol/L HCl and 0.1 mol/L NaOH. After stirring for 5 min, the pulp was allowed to settle for an additional 10 min. Finally, the suspension was collected and used for the measurements. Each measurement was repeated at least five times, and the mean values and standard deviations were recorded.

2.5. Contact Angle Measurements

The contact angles of the digenite samples with different treatments (with DI water; with Na_2S; with Na_2S and SBX; with Fe^{3+}; with Fe^{3+} and Na_2S; with Fe^{3+}, Na_2S and SBX) were measured using a JC2000A (Powereach Instruments, Shanghai, China) contact angle apparatus at approximately 25 °C. The samples were prepared similarly to those for the microflotation experiments and then dried in a vacuum oven at 40 °C. Subsequently, the samples were processed using a tablet press machine to obtain laminar samples with highly smooth surfaces. Finally, the samples were placed in a rectangular glass chamber, and a stable liquid drop was introduced onto their surfaces using a microsyringe. Particular care was taken during the measurements to avoid vibration of the needle and distortion of the drop shape. Each measurement was repeated at least five times, and the mean values and standard deviations were considered.

2.6. XPS Analyses

XPS measurements were conducted using a Thermo Scientific ESCALAB 250 XI spectrometer (Thermo Fisher Scientific, Waltham, MA, USA). The X-ray source was Al Kα (1253.6 eV), operated at 200 W, and the scanned area was 2 mm × 2 mm. The samples used for the XPS measurements were prepared according to microflotation experiments. After being conditioned in the desired solutions, the samples were rinsed with DI water, filtered, and dried in a stream of high-purity nitrogen for XPS measurements. During the tests, the vacuum pressure in the analysis chamber was 8.0×10^{-7} Pa, and the electron take-off angle was 90°. After scanning all the elements in the samples, high-resolution spectra were collected to obtain information about the elemental valence and oxidation states. The

obtained XPS data were processed using Thermo Scientific Avantage 5.52 (Thermo Fisher Scientific, Waltham, MA, USA), and the C 1s peak at 284.8 eV was used as the reference to calibrate the measured binding energies [25].

2.7. Optical Microscopy Analysis

The agglomeration and dispersion behaviors of digenite fine particles with different treatments were observed using an ML 31 biological microscope (Guangzhou Micro-shot Optical Technology Co. Ltd., Guangzhou, China). During sample preparation, 5 g of digenite was mixed with 50 mL of DI water and stirred for 3 min. Then, the desired flotation reagents were added, corresponding to the microflotation experiments. Subsequently, 2 mL of the pulp was extracted using a syringe, transferred to a beaker, and diluted ten times with DI water. Following stirring, the dilute solution was dropped onto a glass slide, which was followed by optical microscopy.

3. Results

3.1. Microflotation Tests

The results of X-ray diffraction (shown in Figure 1) and chemical element analysis showed that the purity of digenite was 98.52%, meeting the testing requirements of this study.

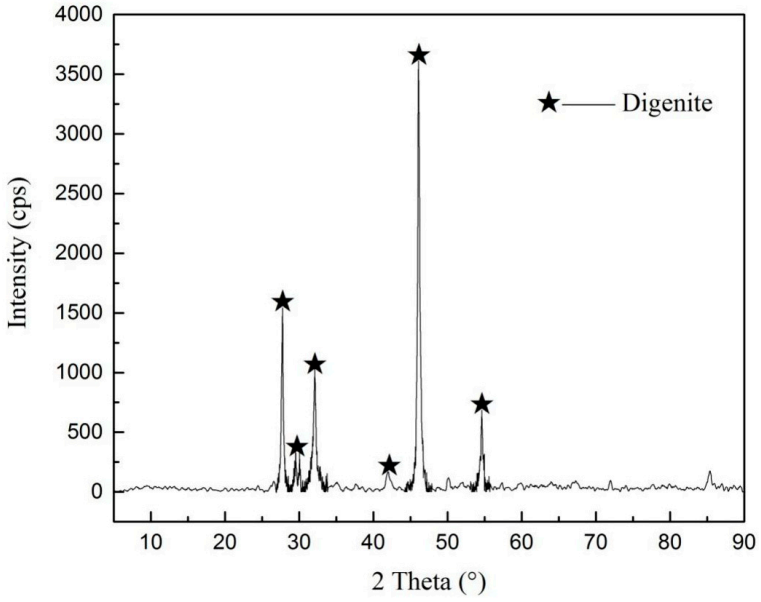

Figure 1. X-ray diffraction pattern of digenite.

The results of the microflotation tests are displayed in terms of the recovery as a function of flotation time under different conditions. The values of the correlation index R^2 for all the microflotation tests were above 0.98 (not shown here), indicating that the flotation results almost exactly matched those of the first-order kinetic model.

Figure 2 shows the effect of Na_2S dosage on the flotation rate and recovery of fine digenite particles at different flotation times. As can be seen, when the digenite fine particles were heavily oxidized, the floatability was extremely low, because of which the recovery at 3 min and the flotation rate constant were only 5.66% and 0.15 min^{-1}, respectively. However, once Na_2S was introduced into the solution, the floatability of the oxidized digenite fine particles increased. When the Na_2S dosage was increased from 0.21×10^{-3} mol/L to 1.25×10^{-3} mol/L, the recovery at 3 min increased from 40.35% to 88.73%, and the flotation rate constant increased from 0.34 to 2.34 min^{-1}. With further addition of Na_2S, the flotation rate constant increased, while the recovery at 3 min reached

a plateau. It can be concluded that a high dosage of Na_2S is beneficial for restoring the floatability of heavily oxidized digenite fine particles.

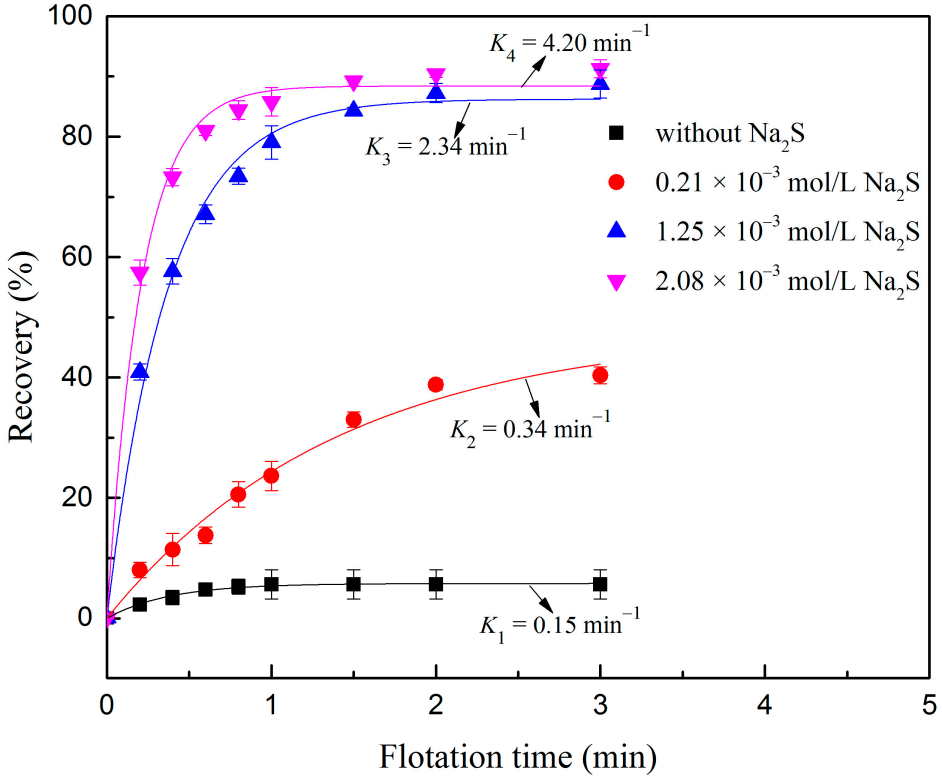

Figure 2. Flotation recovery of digenite as a function of flotation time with respect to Na_2S dosage (pH: 7.0; sodium butyl xanthate (SBX) dosage: 1×10^{-4} mol/L).

The effect of Fe^{3+} dosage on the sulfidization flotation of oxidized digenite fine particles at different flotation times is shown in Figure 3. As can be seen, when Fe^{3+} dosage was 3×10^{-4} mol/L, the recovery at 3 min and the flotation rate constant was 91.26% and 2.46 min^{-1}, respectively. This result was nearly the same as that of oxidized digenite fine particles after sulfidization without the addition of Fe^{3+}, as shown in Figure 2. However, once the Fe^{3+} dosage exceeded 5×10^{-4} mol/L, both the recovery and flotation rate constants significantly decreased. When the Fe^{3+} dosage was 1×10^{-3} mol/L, the recovery and flotation rate constants were only 4.81% and 0.25 min^{-1}, respectively. This indicated that a high dosage of Fe^{3+} was not conducive to the sulfidization flotation of oxidized digenite fine particles. In solutions, Fe^{3+} species can react with xanthate anions to decrease the amount of the effective components of SBX adsorbed on the surface, thus preventing the flotation of sulfide minerals. To clarify whether the depressing effect of Fe^{3+} is relevant to the consumption of SBX, the sulfidization flotation of digenite after adding 1×10^{-3} mol/L Fe^{3+} with decantation treatment was carried out. However, compared with the corresponding values without the decantation treatment, it can be seen that both the recovery and flotation rate constants of digenite only increased to 7.38% and 0.25 min^{-1}, respectively. This indicates that the depressing effect of Fe^{3+} is mainly attributed to the adsorption of Fe^{3+} on the surface of the oxidized digenite fine particles.

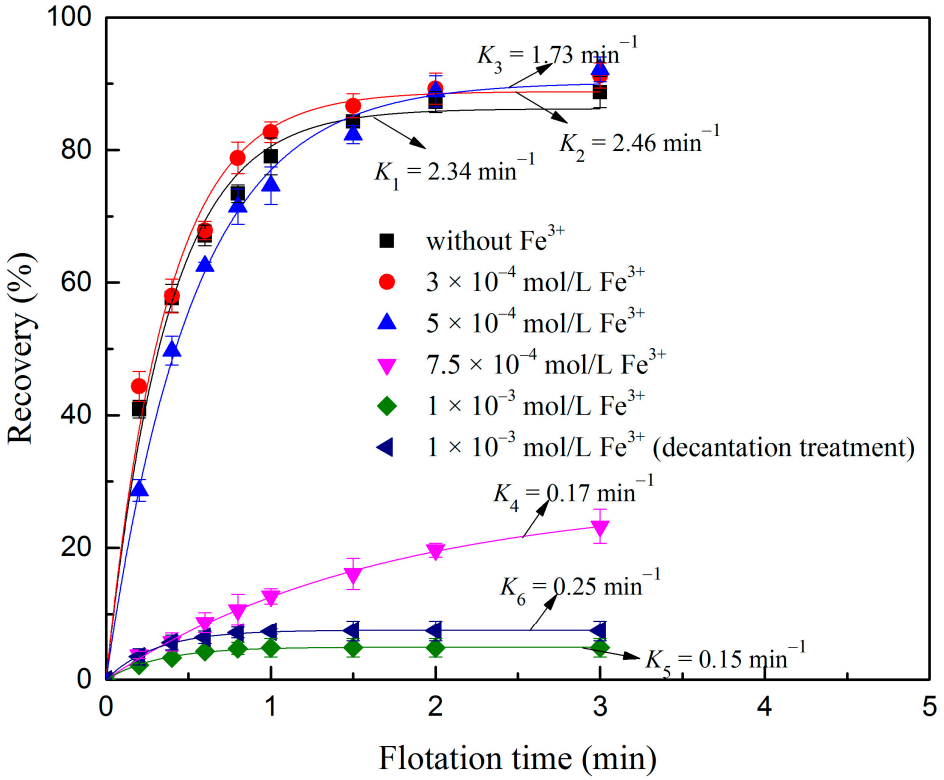

Figure 3. Flotation recovery of digenite as a function of flotation time with respect to Fe^{3+} dosage (pH: 7.0; Na_2S dosage: 1.25 × 10^{-3} mol/L; SBX dosage: 1 × 10^{-4} mol/L).

3.2. Fe^{3+} Adsorption Experiments

To verify that Fe^{3+} can be adsorbed on the surface of oxidized digenite fine particles, the adsorption amount of Fe^{3+} was measured; the results are shown in Figure 4. As seen in the figure, the adsorption amount and initial Fe^{3+} concentration were linearly correlated. When the initial Fe^{3+} concentration was increased from 1 × 10^{-4} to 1 × 10^{-3} mol/L, the adsorption amount significantly increased from 1.85 × 10^{-6} to 17.95 × 10^{-6} mol/g. Therefore, when the Fe^{3+} concentration was 1 × 10^{-3} mol/L during the flotation, the residual Fe^{3+} concentration in the solution was negligible. The suppressing effect of Fe^{3+} can be attributed mainly to the adsorption of Fe^{3+} on the surface of oxidized digenite fine particles.

3.3. Zeta Potential Measurements

Zeta potential measurements reflect the interaction mode and intensity between the reagents and the mineral surface [26,27]. As shown in Figure 5, as the pH increased, the zeta potential values of the oxidized digenite first increased and then decreased. The isoelectric point (IEP) was found at pH 7.4 and 9.30; these values are similar to those for copper oxides/hydroxides [28]. However, when digenite was treated with Na_2S, the zeta potential values in the measured pH range significantly decreased to more negative values, which was mainly because of the chemisorption of HS^- hydrolyzed from Na_2S on the digenite surface. With the further addition of SBX, the zeta potential values shifted to more negative values, indicating that negatively charged xanthate ions were adsorbed on the digenite surface after treatment with Na_2S.

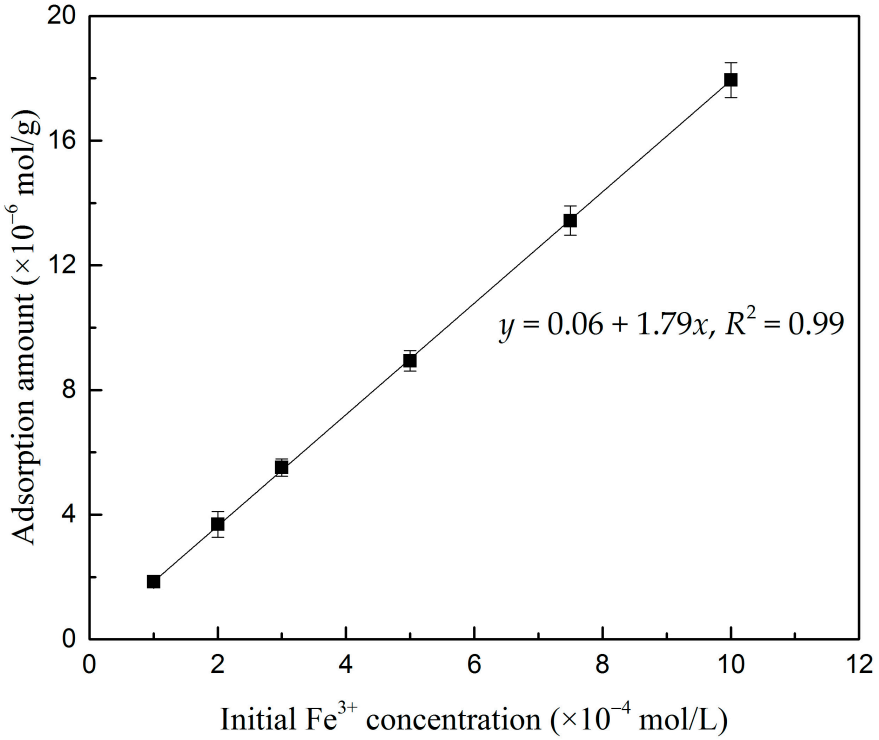

Figure 4. Adsorption amount of Fe^{3+} on digenite surface as a function of the initial Fe^{3+} concentration at pH 7.0.

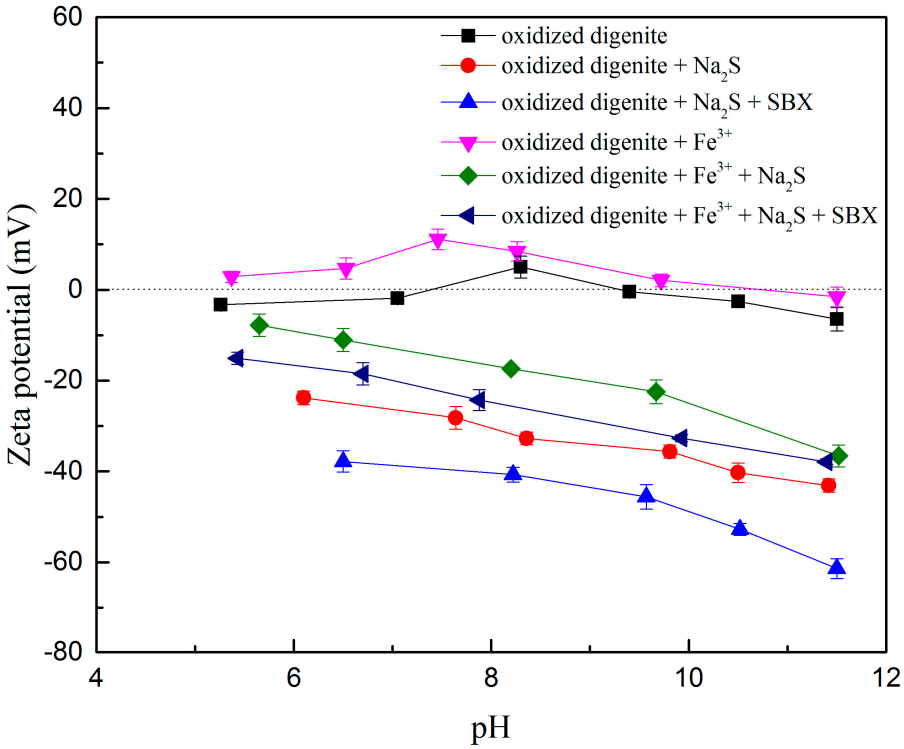

Figure 5. Zeta potentials of oxidized digenite as a function of pH with different treatments (Fe^{3+} dosage: 1×10^{-3} mol/L; Na_2S dosage: 1.25×10^{-3} mol/L; SBX dosage: 1×10^{-4} mol/L).

However, once Fe^{3+} was added to the solution, the zeta potential of oxidized digenite shifted to more positive values, and the IEP became pH 10.8. Based on the distribution diagram of the 1×10^{-3} mol/L Fe^{3+} shown in Figure 6, Fe^{3+} exists in the solutions in various forms at different pH values. When the pH is less than 2.06, the dissociated Fe^{3+}

is the main species; the amounts of other species gradually increase as the pH increases. When the pH was greater than 2.06, the amount of positively charged species (especially Fe^{3+}) gradually decreased as the pH increased, and $Fe(OH)_3$ particles became the dominant species. Therefore, Fe^{3+} was mainly absorbed on the digenite surface in the form of $Fe(OH)_3$ particles at pH 7.0, and the zeta potential increased at this pH because of the electrostatic adsorption of $Fe(OH)_2^+$ and $Fe(OH)^{2+}$ on the surface. After the addition of Na_2S, the zeta potential values shifted to between −7.8 and −36.6 mV at pH 5.6–11.5, indicating intense chemisorption of HS^- on the surface. However, with further addition of SBX, the declining trend of the zeta potential values in the measured pH range was not evident, indicating that weak chemisorption of xanthate ions had occurred on the surface. This also demonstrated that the presence of Fe^{3+} hinders effective adsorption of SBX on the surface of oxidized digenite fine particles after sulfidization, thus reducing the recovery and flotation rate of the mineral.

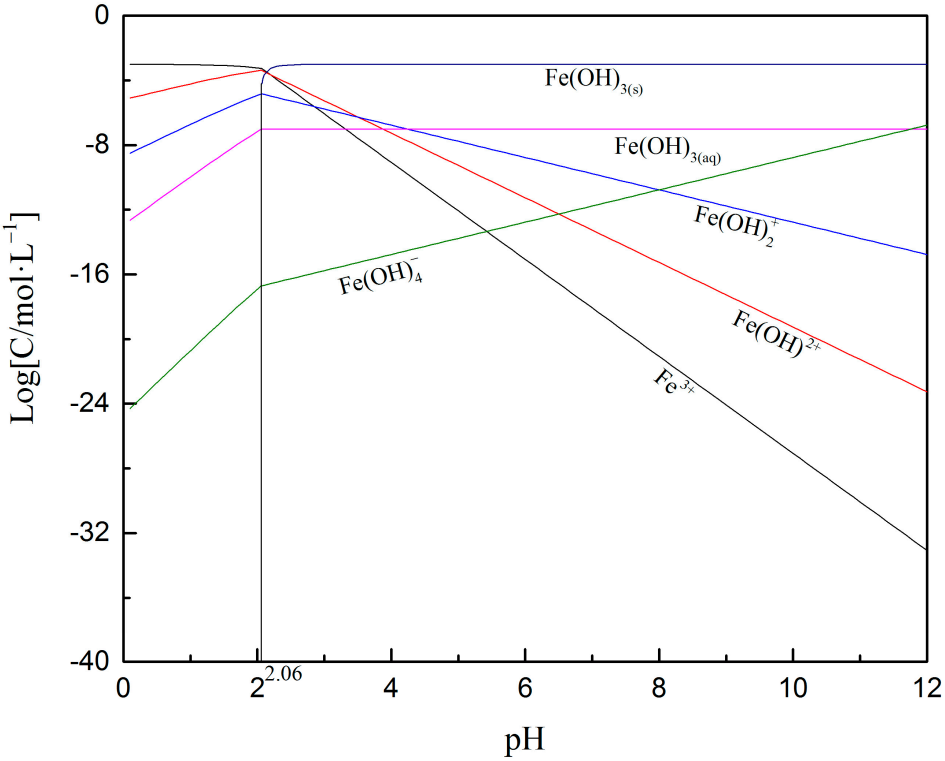

Figure 6. Species distribution diagram of 1×10^{-3} mol/L Fe^{3+} in the solution as a function of pH [29].

3.4. Contact Angle Measurements

The contact angles of the oxidized digenite fine particles with different treatments in the absence and presence of Fe^{3+} are shown in Figure 7. For the samples without the addition of Fe^{3+}, after the digenite fine particles were heavily oxidized, the contact angle was 8.6°; this indicates that the surface of digenite was nearly completely hydrophilic. After Na_2S was added, the contact angle increased to 53.3°. With further addition of SBX, the surface hydrophobicity significantly increased, and the contact angle became 92.4°. This was the main reason that the addition of Na_2S and SBX could restore the floatability of heavily oxidized digenite fine particles. However, once Fe^{3+} was introduced into the solution, the contact angles of digenite with different treatments decreased. When Na_2S and SBX were added, the contact angle was 31.7°, which is far less than that of the sample without the addition of Fe^{3+}. This indicates that the adsorption of Fe^{3+} reduced the surface hydrophobicity of digenite with different treatments, which further decreased in its floatability.

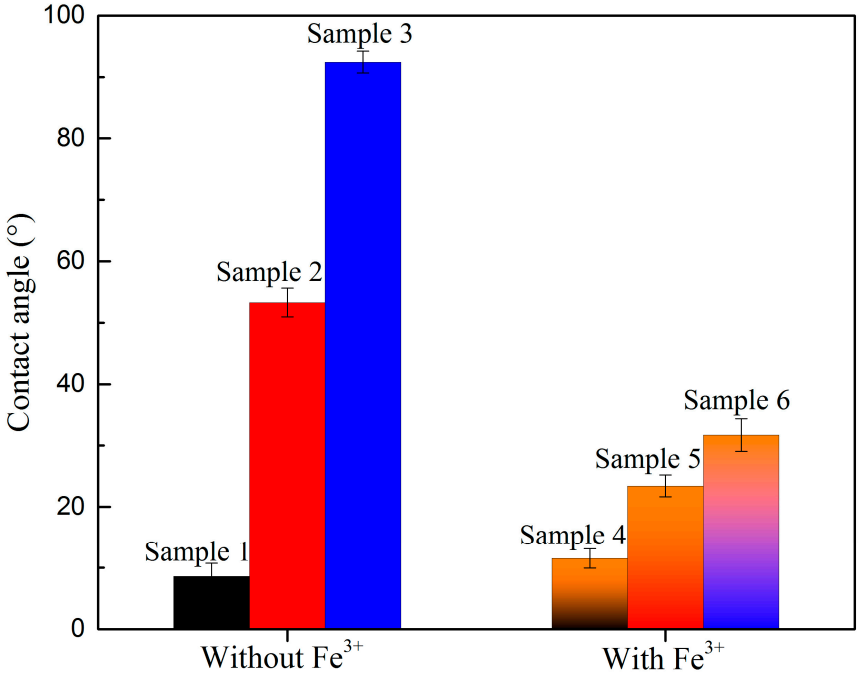

Figure 7. Contact angle of oxidized digenite fine particles with different treatments (Sample 1: with DI water; Sample 2: with 1.25 × 10^{-3} mol/L Na_2S; Sample 3: with 1.25 × 10^{-3} mol/L Na_2S + 1 × 10^{-4} mol/L SBX; Sample 4: with 1 × 10^{-3} mol/L Fe^{3+}; Sample 5: with 1 × 10^{-3} mol/L Fe^{3+} + 1.25 × 10^{-3} mol/L Na_2S; Sample 6: with 1 × 10^{-3} mol/L Fe^{3+} + 1.25 × 10^{-3} mol/L Na_2S + 1 × 10^{-4} mol/L SBX).

3.5. XPS Analysis

To further investigate the reasons for the changes in the surface hydrophobicity and floatability of digenite with different treatments, the chemical species and state on the surface of digenite were analyzed via XPS; the results are displayed in Figures 8 and 9 and Tables 1–5.

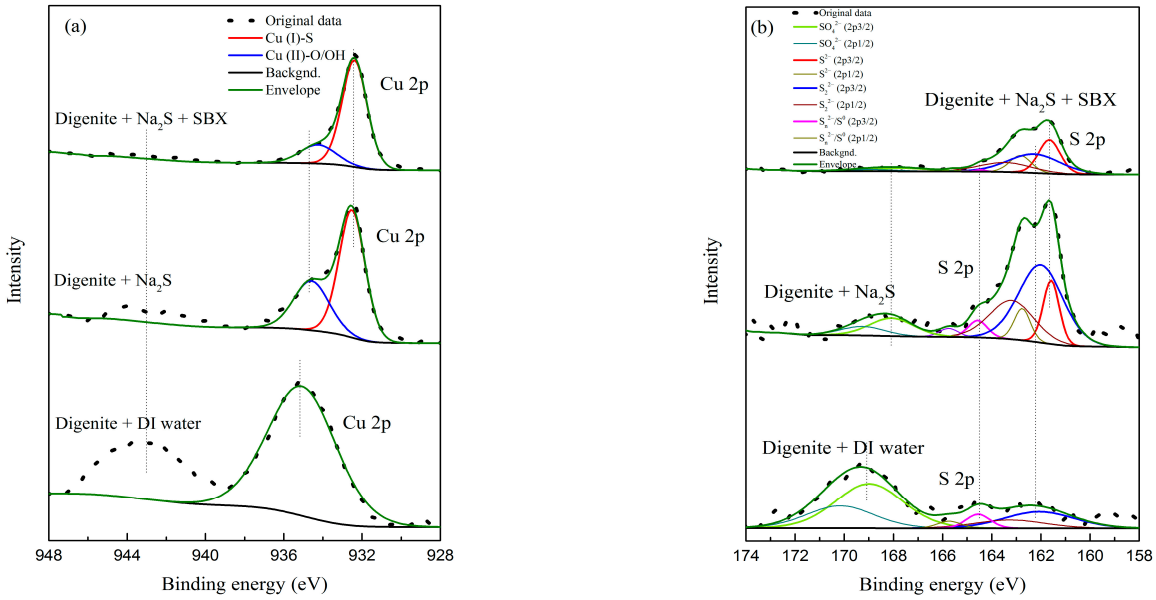

Figure 8. Fitting peaks of Cu 2p (**a**) and S 2p (**b**) for digenite with different treatments in the absence of Fe^{3+} (pH: 7.0; Na_2S dosage: 1.25 × 10^{-3} mol/L; SBX dosage: 1 × 10^{-4} mol/L).

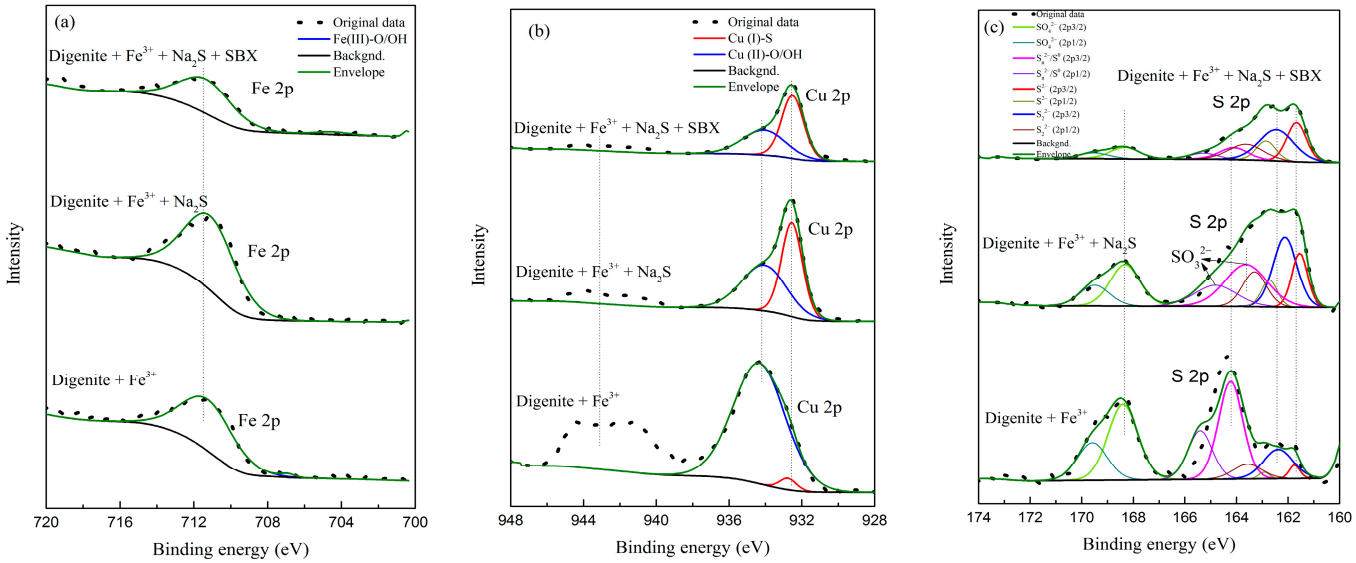

Figure 9. Fitting peaks of Fe 2p (**a**), Cu 2p (**b**), and S 2p (**c**) for digenite with different treatments in the presence of Fe^{3+} (pH: 7.0; Fe^{3+} dosage: 1×10^{-3} mol/L; Na_2S dosage: 1.25×10^{-3} mol/L; SBX dosage: 1×10^{-4} mol/L).

Table 1. Cu 2p quantification of digenite with different treatments in the absence of Fe^{3+}.

Species	DI Water		Na_2S		Na_2S + SBX	
	B.E.	at.%	B.E.	at.%	B.E.	at.%
Cu (I)-S	-	-	932.51	65.61	932.39	89.01
Cu (II)-O/OH	935.07	100.00	934.59	34.39	934.24	10.99

Note: DI represents Deionized; B.E. represents Binding Energy; at.% represnts atomic percentage content.

Table 2. S 2p quantification of digenite with different treatments in the absence of Fe^{3+}.

Species	DI Water		Na_2S		Na_2S + SBX	
	B.E. (eV)	at. (%)	B.E. (eV)	at. (%)	B.E. (eV)	at. (%)
S^{2-}	161.51/162.69	-	161.58/162.76	18.36	161.65/162.83	37.94
S_2^{2-}	162.07/163.25	25.71	162.00/163.18	61.56	162.26/163.44	51.40
S_n^{2-}/S^0	164.55/165.73	7.47	164.57/165.75	5.82	164.44/165.62	0.94
SO_4^{2-}	168.98/170.16	66.83	168.07/169.25	14.25	167.70/168.88	9.73

Table 3. Fe 2p quantification of digenite with different treatments in the presence of Fe^{3+}.

Species	Fe^{3+}		Fe^{3+} + Na_2S		Fe^{3+} + Na_2S + SBX	
	B.E. (eV)	at. (%)	B.E. (eV)	at. (%)	B.E. (eV)	at. (%)
Fe(II)-S	707.13	-	707.13	-	707.13	-
Fe(III)-O/OH	711.10	100.00	711.75	100.00	711.33	100.00

Table 4. Cu 2p quantification of digenite with different treatments in the presence of Fe^{3+}.

Species	Fe^{3+}		Fe^{3+} + Na_2S		Fe^{3+} + Na_2S + SBX	
	B.E. (eV)	at. (%)	B.E. (eV)	at. (%)	B.E. (eV)	at. (%)
Cu (I)-S	932.76	2.94	932.54	49.02	932.52	58.98
Cu (II)-O/OH	934.34	97.06	934.06	50.98	934.16	41.02

Table 5. S 2p quantification of digenite with different treatments in the presence of Fe^{3+}.

Species	Fe^{3+}		Fe^{3+} + Na_2S		Fe^{3+} + Na_2S + SBX	
	B.E. (eV)	at. (%)	B.E. (eV)	at. (%)	B.E. (eV)	at. (%)
S^{2-}	161.75/162.93	2.54	161.55/162.73	15.41	161.67/162.85	30.08
S_2^{2-}	162.38/163.56	15.33	162.12/163.30	30.01	162.45/163.63	42.88
SO_3^{2-}	-	-	163.63/164.81	32.18	-	-
S_n^{2-}/S^0	164.22/165.40	42.00	-	-	164.10/165.28	13.61
$SO4^{2-}$	168.40/169.58	40.14	168.32/169.50	22.41	168.33/169.51	13.43

Figure 8a and Table 1 display the high-resolution spectra of Cu 2p3/2 and the corresponding species amounts for digenite samples in the absence of Fe^{3+}. The peaks centered at 932.51 and 934.59 eV are assigned to Cu(I)-S and Cu(II)-O/OH species, respectively [30,31]. The low-intensity broad satellite peak centered at 943.01 eV indicates that the surfaces of sulfide minerals were heavily oxidized [32,33]. After digenite was heavily oxidized, only hydrophilic Cu(II)-O/OH species were detected on the surface, which was the main reason that both the recovery and flotation rate constant were extremely low. However, as Na_2S was added to the solution, the amount of Cu(II)-O/OH species significantly decreased to 34.39%, and the Cu(I)-S species became the major component on the surface. Further addition of SBX reduced the amount of Cu(II)-O/OH species to 10.99%, and the satellite peak at 943.01 eV almost disappeared; this indicates that almost all hydrophilic species had been converted to Cu(I)-S species because of the oxidation of xanthate anions (X^-). Thus, the surface hydrophobicity of digenite increased, and the samples could be effectively recovered, which is consistent with the microflotation results shown in Figure 2.

Figure 8b and Table 2 show the high-resolution spectra of S 2p and corresponding species amounts for digenite samples in the absence of Fe^{3+}, which were fitted using the 2p1/2 and 2p3/2 peaks with a 1:2 area ratio and 1.18 eV splitting energy [34]. The S 2p3/2 XPS spectra can be mainly divided into four peaks at 161.51, 162.07, 164.55, and 168.98 eV, which can be assigned to monosulfides (S^{2-}), disulfides (S_2^{2-}), polysulfides/elemental sulfur (S_n^{2-}/S^0), and sulfates (SO_4^{2-}), respectively [35]. After treatment with Na_2S and SBX, S_2^{2-} became the main species on the surface of digenite, which could be attributed to the adsorption of S^{2-} and the dissolution of hydrophilic SO_4^{2-} species. Previous studies have shown that hydrophobic S_n^{2-}/S^0 species are beneficial for the flotation of sulfide minerals [36]. As shown in Table 2, the amount of S_n^{2-}/S^0 species on the digenite surface treated with DI water was 7.47%, which was higher than that of the samples treated with Na_2S and SBX. Combined with the analysis result of Cu 2p3/2, the optimal floatability of digenite after treatment with Na_2S and SBX could mainly be attributed to the minimum amount of hydrophilic Cu(II)-O species on the surface.

Figure 9 and Tables 3–5 illustrate the high-resolution spectra and corresponding species amounts based on the decoupling of Fe 2p, Cu 2p, and S 2p for digenite samples in the presence of Fe^{3+}. Based on the previous literature, the Fe 2p3/2 spectrum can be divided into two spectral peaks at approximately 707 and 711 eV, which are assigned to Fe(II)-S and Fe(III)-O/OH species, respectively [37,38]. However, as shown in Figure 9a, only the peaks at 711.10 eV were detected on the surface with different treatments. Combined with the species distribution diagram of Fe^{3+} shown in Figure 6, Fe^{3+} was adsorbed on the surface of digenite mainly in the form of $Fe(OH)_3$. From the decoupling results of Cu 2p, it can be seen that after digenite was treated with Fe^{3+}, only 2.94% Cu(I)-S species were detected, and the hydrophilic Cu(II)-O/OH species were still the main components on the surface. In addition, the satellite peak centered at 943.01 eV could also be clearly observed. After the digenite was treated with Fe^{3+} and Na_2S, the Cu(II)-O/OH species significantly decreased to 50.98%, which is significantly higher than that after treatment with Na_2S alone, as shown in Table 1. This indicates that the adsorption of Fe^{3+} is not beneficial for the effective sulfidization of digenite. Subsequently, with the further addition of SBX, the amount of Cu(II)-O/OH species slightly decreased to 41.02%. This is because

the Fe(III)-O/OH species on the surface have a weak interaction with X^-, preventing the effective adsorption of X^- on the digenite surface [39]. From the decoupling results of S 2p, it was found that the amount of S_n^{2-}/S^0 species was 13.61% after treatment with Fe^{3+}, Na_2S, and SBX, which was higher than the amounts found in the absence of Fe^{3+}. Therefore, the poor floatability of digenite in the presence of Fe^{3+} was attributed to the production of large amounts of hydrophilic iron and copper oxides/hydroxides.

3.6. Optical Microscopy Analysis

It has been confirmed that the effective recovery of fine metal sulfide mineral particles (such as galena, sphalerite, and pyrite) is directly related to the formation of hydrophobic agglomerates, which can be induced by adding xanthates [40–42]. The agglomeration and dispersion behaviors of fine mineral particles are usually assessed by optical microscopy analysis.

As shown in Figure 10, oxidized digenite fine particles without any treatment are well dispersed in DI water. It is well known that the hydrophobic agglomeration of fine particles is mainly dependent on the surface hydrophobicity of minerals. When digenite fine particles are heavily oxidized, the surface of digenite is strongly hydrophilic, and the interactions between fine particles are determined by the electric double layer force. As the zeta potential value on the surface of digenite was negative at pH 7.0, the electrostatic repulsive forces resulted in good dispersion of fine particles in the solution. However, when digenite was treated with Na_2S and SBX, it can be seen that large sized agglomerates formed. Based on the results shown in Figure 5, the zeta potential value on the surface of digenite after treatment with Na_2S and SBX was strongly negative at pH 7.0, indicating that the electrical interactions between particles were repulsive. However, as the addition of Na_2S and SBX decreased the amount of hydrophilic species and significantly increased the surface hydrophobicity of digenite, the formation of agglomerates could mainly be attributed to the strong hydrophobic attractive forces. Moreover, instead of individual fine particles, the large hydrophobic agglomerates interacted with the bubbles, thus increasing the collision probability between the particles and bubbles and promoting effective recovery of digenite fine particles. However, after Fe^{3+} was introduced into the pulp, the particles were well dispersed, which was also due to the repulsive electrostatic forces between the digenite fine particles.

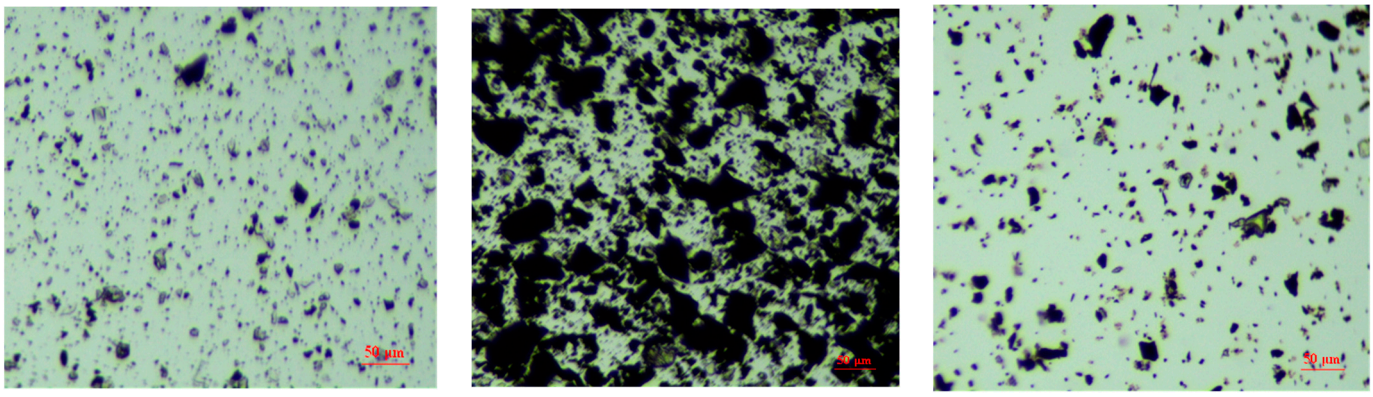

(**a**) (**b**) (**c**)

Figure 10. Microscopy images of oxidized digenite fine particles with different treatments (**a**) with deionized (DI) water; (**b**) with 1.25×10^{-3} mol/L Na_2S + 1×10^{-4} mol/L SBX; (**c**) with 1×10^{-3} mol/L Fe^{3+} + 1.25×10^{-3} mol/L Na_2S + 1×10^{-4} mol/L SBX).

4. Conclusions

This study investigated the effect of Fe^{3+} on the sulfidization flotation performance of oxidized digenite fine particles and the underlying mechanism. The main conclusions and research significance are summarized as follows:

1. A low dosage of Fe^{3+} had no significant effect on the sulfidization flotation of oxidized digenite fine particles. However, as the Fe^{3+} dosage exceeded 5×10^{-4} mol/L, both the flotation rate and recovery of digenite significantly decreased.
2. Fe^{3+} can adsorb on the surface of oxidized digenite fine particles mainly in the form of hydrophilic $Fe(OH)_3$ species, hindering the effective sulfidization of digenite, which decreases the surface hydrophobicity, and further prevents the flotation recovery of digenite.
3. With the addition of Na_2S and SBX, a remarkable agglomeration performance of oxidized digenite fine particles was observed, which was the main reason for the good floatability of digenite. However, the presence of Fe^{3+} prevents the formation of hydrophobic agglomerates, resulting in a low flotation rate and recovery of digenite.
4. This study is of great significance for realizing the effective separation of oxidized digenite fine particles and iron sulfide minerals. When the amount of Fe^{3+} dissolved from oxidized iron sulfide minerals is less than a critical value, digenite can be recovered using sulfidization technology. However, once the dissolved Fe^{3+} exceeds the critical value, measurements must be taken before sulfidization to desorb the Fe^{3+} species adsorbed on the surface and decrease the amount of Fe^{3+} in the pulp.

Author Contributions: Methodology, J.X., S.W. and X.B.; validation, J.X. and S.W.; investigation, D.R. and T.C.; resources, J.X., X.B., Z.S. and C.Z.; data curation, J.X. and X.B.; writing—original draft preparation, J.X.; writing—review and editing, S.W. and Z.S.; supervision, X.B.; funding acquisition, J.X. and X.B. All authors have read and agreed to the published version of the manuscript.

Funding: This research was funded by Open Foundation of State Key Laboratory of Mineral Processing (BGRIMM-KJSKL-2021-19), the Talent Science and Technology Fund of Xi'an University of Architecture and Technology (ZR19062), and the National Natural Science Foundation of China (52074206).

Institutional Review Board Statement: Not applicable.

Informed Consent Statement: Not applicable.

Data Availability Statement: Not applicable.

Conflicts of Interest: The authors declare no conflict of interest.

References

1. Schipper, B.W.; Lin, H.C.; Meloni, M.A.; Wansleeben, K.; Heijungs, R.; van der Voet, E. Estimating global copper demand until 2100 with regression and stock dynamics. *Resour. Conserv. Recycl.* **2018**, *132*, 28–36. [CrossRef]
2. Liu, S.; Zhang, Y.; Su, Z.; Lu, M.; Gu, F.; Liu, J.; Jiang, T. Recycling the domestic copper scrap to address the China's copper sustainability. *J. Mater. Res. Technol.* **2020**, *9*, 2846–2855. [CrossRef]
3. Bilal, M.; Ito, M.; Koike, K.; Hornn, V.; Ul Hassan, F.; Jeon, S.; Park, I.; Hiroyoshi, N. Effects of coarse chalcopyrite on flotation behavior of fine chalcopyrite. *Miner. Eng.* **2021**, *163*, 106776. [CrossRef]
4. Yin, W.; Tang, Y. Interactive effect of minerals on complex ore flotation: A brief review. *Int. J. Miner. Metall. Mater.* **2020**, *27*, 571–583. [CrossRef]
5. Sivamohan, R. The problem of recovering very fine particles in mineral processing—A review. *Int. J. Miner. Process.* **1990**, *28*, 247–288. [CrossRef]
6. Subrahmanyam, T.V.; Forssberg, K.S.E. Fine particles processing: Shear-flocculation and carrier flotation—A review. *Int. J. Miner. Process.* **1990**, *30*, 265–286. [CrossRef]
7. Finkelstein, N.P. Addendum to: The activation of sulphide minerals for flotation: A review. *Int. J. Miner. Process.* **1999**, *55*, 283–286. [CrossRef]
8. Deng, J.; Wen, S.; Xian, Y.; Liu, J.; Bai, S. New discovery of unavoidable ions source in chalcopyrite flotation pulp: Fluid inclusions. *Miner. Eng.* **2013**, *42*, 22–28. [CrossRef]
9. Bai, S.; Wen, S.; Xian, Y.; Liu, J.; Deng, J. New source of unavoidable ions in galena flotation pulp: Components released from fluid inclusions. *Miner. Eng.* **2013**, *45*, 94–99. [CrossRef]

10. Peng, Y.; Grano, S.; Fornasiero, D.; Ralston, J. Control of grinding conditions in the flotation of galena and its separation from pyrite. *Int. J. Miner. Process.* **2003**, *70*, 67–82. [CrossRef]
11. Ma, Y.; Huang, F.; Yin, W.; Tang, Y.; Zhang, S. Influence and mechanism of Fe^{3+} on flotation of digenite. *Chin. J. Nonferrous Met.* **2018**, *28*, 817–822. (In Chinese)
12. Liu, R.; Liu, D.; Li, J.; Li, J.; Liu, Z.; Jia, X.; Yang, S.; Li, J.; Ning, S. Sulfidization mechanism in malachite flotation: A heterogeneous solid-liquid reaction that yields Cu_xS_y phases grown on malachite. *Miner. Eng.* **2020**, *154*, 106420. [CrossRef]
13. Wang, H.; Wen, S.; Han, G.; Feng, Q. Applied Surface Science Modification of malachite surfaces with lead ions and its contribution to the sulfidization flotation. *Appl. Surf. Sci.* **2021**, *550*, 149350. [CrossRef]
14. Zhang, Q.; Wen, S.; Feng, Q.; Liu, J. Surface modification of azurite with lead ions and its effects on the adsorption of sulfide ions and xanthate species. *Appl. Surf. Sci.* **2021**, *543*, 148795. [CrossRef]
15. Liu, R.; Liu, D.; Li, J.; Liu, S.; Liu, Z.; Gao, L.; Jia, X.; Ao, S. Improved understanding of the sulfidization mechanism in cerussite flotation: An XPS, ToF-SIMS and FESEM investigation. *Colloids Surf. A* **2020**, *595*, 124508. [CrossRef]
16. Orwe, D.; Grano, S.R.; Lauder, D.W. Increasing fine copper recovery at the Ok Tedi concentrator, Papua New Guinea. *Miner. Eng.* **1998**, *11*, 171–187. [CrossRef]
17. Newell, A.J.H.; Skinner, W.M.; Bradshaw, D.J. Restoring the floatability of oxidised sulfides using sulfidisation. *Int. J. Miner. Process.* **2007**, *84*, 108–117. [CrossRef]
18. Moimane, T.; Huai, Y.; Peng, Y. Evaluating the sulphidisation and flotation of oxidised chalcopyrite. *Miner. Eng.* **2021**, *164*, 106816. [CrossRef]
19. Cao, Z.; Chen, X.; Peng, Y. The role of sodium sulfide in the flotation of pyrite depressed in chalcopyrite flotation. *Miner. Eng.* **2018**, *119*, 93–98. [CrossRef]
20. Xu, M. Modified flotation rate constant and selectivity index. *Miner. Eng.* **1998**, *11*, 271–278. [CrossRef]
21. Zhang, N.; Zhou, C.; Liu, C.; Pan, J.; Tang, M.; Cao, S.; Ouyang, C.; Peng, C. Bin Effects of particle size on flotation parameters in the separation of diaspore and kaolinite. *Powder Technol.* **2017**, *317*, 253–263. [CrossRef]
22. Natarajan, R.; Nirdosh, I. Effect of molecular structure on the kinetics of flotation of a Canadian nickel ore by N-arylhydroxamic acids. *Int. J. Miner. Process.* **2009**, *93*, 284–288. [CrossRef]
23. Yao, J.; Sun, H.; Han, F.; Yin, W.; Hong, J.; Wang, Y.; Won, C.; Du, L. Enhancing selectivity of modifier on magnesite and dolomite surfaces by pH control. *Powder Technol.* **2020**, *362*, 698–706. [CrossRef]
24. Li, Z.; Han, Y.; Gao, P.; Wang, H.; Liu, J. The interaction among multiple charged particles induced by cations and direct force measurements by AFM. *Colloids Surf. A* **2020**, *589*, 124440. [CrossRef]
25. Yang, B.; Yin, W.; Zhu, Z.; Sun, H.; Sheng, Q.; Fu, Y.; Yao, J.; Zhao, K. Differential adsorption of hydrolytic polymaleic anhydride as an eco-friendly depressant for the selective flotation of apatite from dolomite. *Sep. Purif. Technol.* **2021**, *256*, 117803. [CrossRef]
26. Liu, W.; Liu, W.; Wang, B.; Duan, H.; Peng, X.; Chen, X.; Zhao, Q. Novel hydroxy polyamine surfactant N-(2-hydroxyethyl)-N-dodecyl-ethanediamine: Its synthesis and flotation performance study to quartz. *Miner. Eng.* **2019**, *142*, 105894. [CrossRef]
27. Zhu, Z.; Wang, D.; Yang, B.; Yin, W.; Ardakani, M.S.; Yao, J.; Drelich, J.W. Effect of nano-sized roughness on the flotation of magnesite particles and particle-bubble interactions. *Miner. Eng.* **2020**, *151*, 106340. [CrossRef]
28. Fullston, D.; Fornasiero, D.; Ralston, J. Zeta potential study of the oxidation of copper sulfide minerals. *Colloids Surf. A* **1999**, *146*, 113–121. [CrossRef]
29. Wang, D.; Hu, Y. *Solution Chemistry of Flotation*; Hunan Science and Technology Press: Changsha, China, 1988; pp. 132–134.
30. Dong, J.; Liu, Q.; Yu, L.; Subhonqulov, S.H. The interaction mechanism of Fe^{3+} and NH^{4+} on chalcopyrite surface and its response to flotation separation of chalcopyrite from arsenopyrite. *Sep. Purif. Technol.* **2021**, *256*, 117778. [CrossRef]
31. Moimane, T.; Huai, Y.; Peng, Y. The critical degree of bornite surface oxidation in flotation. *Miner. Eng.* **2020**, *155*, 106445. [CrossRef]
32. Moimane, T.; Plackowski, C.; Peng, Y. The critical degree of mineral surface oxidation in copper sulphide flotation. *Miner. Eng.* **2020**, *145*, 106075. [CrossRef]
33. Hirajima, T.; Miki, H.; Suyantara, G.P.W.; Matsuoka, H.; Elmahdy, A.M.; Sasaki, K.; Imaizumi, Y.; Kuroiwa, S. Selective flotation of chalcopyrite and molybdenite with H_2O_2 oxidation. *Miner. Eng.* **2017**, *100*, 83–92. [CrossRef]
34. Liu, J.; Liu, G.; Yang, X.; Dong, Y.; Zhang, Z. 6-Hexyl-1,2,4,5-tetrazinane-3-thione: Flotation selectivity and mechanism to copper sulfide mineral. *Miner. Eng.* **2020**, *152*, 106345. [CrossRef]
35. Yu, L.; Liu, Q.; Li, S.; Deng, J.; Luo, B.; Lai, H. Depression mechanism involving Fe^{3+} during arsenopyrite flotation. *Sep. Purif. Technol.* **2019**, *222*, 109–116. [CrossRef]
36. Cao, Z.; Wang, P.; Zhang, W.; Zeng, X.; Cao, Y. Mechanism of sodium sulfide on flotation of cyanide-depressed pyrite. *Trans. Nonferrous Met. Soc. China* **2020**, *30*, 484–491. [CrossRef]
37. Mikhlin, Y.; Karacharov, A.; Tomashevich, Y.; Shchukarev, A. Cryogenic XPS study of fast-frozen sulfide minerals: Flotation-related adsorption of n-butyl xanthate and beyond. *J. Electron Spectros. Relat. Phenom.* **2016**, *206*, 65–73. [CrossRef]
38. Tian, M.; Liu, R.; Gao, Z.; Chen, P.; Han, H.; Wang, L.; Zhang, C.; Sun, W.; Hu, Y. Activation mechanism of Fe (III) ions in cassiterite flotation with benzohydroxamic acid collector. *Miner. Eng.* **2018**, *119*, 31–37. [CrossRef]
39. Niu, X.; Chen, J.; Li, Y.; Xia, L.; Li, L.; Sun, H.; Ruan, R. Correlation of surface oxidation with xanthate adsorption and pyrite flotation. *Appl. Surf. Sci.* **2019**, *495*, 143411. [CrossRef]

40. Song, S.; Lopez-Valdivieso, A.; Reyes-Bahena, J.L.; Bermejo-Perez, H.I.; Trass, O. Hydrophobic flocculation of galena fines in aqueous suspensions. *J. Colloid Interface Sci.* **2000**, *227*, 272–281. [CrossRef] [PubMed]
41. Song, S.; Lopez-Valdivieso, A.; Reyes-Bahena, J.L.; Bermejo-Perez, H.I. Hydrophobic flocculation of sphalerite fines in aqueous suspensions induced by ethyl and amyl xanthates. *Colloids Surf. A* **2001**, *181*, 159–169. [CrossRef]
42. Cheng, W.; Deng, Z.; Tong, X.; Lu, T. Hydrophobic agglomeration of fine pyrite particles induced by flotation reagents. *Minerals* **2020**, *10*, 801. [CrossRef]